High-order variational perturbation theory for the free energy

Florian Weissbach,* Axel Pelster,† and Bodo Hamprecht‡
Institut für Theoretische Physik, Freie Universität Berlin, Arnimallee 14, 14195 Berlin, Germany
(Received 6 March 2002; published 25 September 2002)

In this paper we introduce a generalization to the algebraic Bender-Wu recursion relation for the eigenvalues and the eigenfunctions of the anharmonic oscillator. We extend this well known formalism to the time-dependent quantum statistical Schrödinger equation, thus obtaining the imaginary-time evolution amplitude by solving a recursive set of ordinary differential equations. This approach enables us to evaluate global and local quantum statistical quantities of the anharmonic oscillator to much higher orders than by evaluating Feynman diagrams. We probe our perturbative results by deriving a perturbative expression for the free energy, which is then subject to variational perturbation theory as developed by Kleinert, yielding convergent results for the free energy for all values of the coupling strength.

DOI: 10.1103/PhysRevE.66.036129 PACS number(s): 05.30.−d

I. INTRODUCTION

Most physical problems can only be solved by approximation methods. One of them is perturbation theory that yields weak-coupling expansions. Unfortunately, they often do not converge.

The ground state energy of the anharmonic oscillator is the simplest example where this phenomenon can be studied. Algebraic recursion relations as proposed by Bender and Wu [1] yield perturbation series for the eigenvalues (energies) and eigenfunctions (wave functions) of the time-independent Schrödinger equation up to arbitrarily high orders. In Ref. [2] the calculation was extended to 250th order. The Bender-Wu recursion relation yields a power series for the anharmonic part of the wave function both in the coupling strength g and in the coordinate x. The power series in x can be cut off naturally by comparing the recursive results with those obtained from evaluating Feynman diagrams. The resulting weak-coupling series for the ground state energy does not converge for any value of the coupling strength. This paper deals with both problems: Obtaining high-order perturbation expressions and making them converge for all values of the coupling strength. This paper is organized as follows.

In Sec. II we perturbatively evaluate the path integral representation for the imaginary-time evolution amplitude of the anharmonic oscillator by means of a generalized Wick's theorem [3,4]. In Sec. III we represent the first-order results diagrammatically. Doing so, we demonstrate that the algebraic computational cost is very high for the diagrammatic approach. We also obtain a cross check for the results that are derived from a differential recursion relation in Sec. IV. In order to cut down on the algebraic computational cost we introduce a strategy to exploit the symmetry property of the imaginary-time evolution amplitude in Sec. V, thus laying the foundation for our high-order results. In Sec. VI we combine the resulting algebraic recursion relation with the original differential recursion relation, thus generalizing the Bender-Wu approach [1]. From our perturbative results for the imaginary-time evolution amplitude we then gain a perturbation expression for the free energy of the anharmonic oscillator in Sec. VII, which we check again diagrammatically in Sec. VIII. The perturbative results are then resummed in Sec. IX by means of variational perturbation theory [5] for intermediate coupling $g=1$ for which the usual weak-coupling series would diverge. This theory is a systematic extension of a simple variational approach, first developed by Feynman and Kleinert in the path integral formalism. Feynman introduced the path integral formalism as a quantization regulation, that represents the operator properties of quantum physics by fluctuations of the dynamical variables [6,7]. By extending analytically real time to imaginary time, also quantum statistical quantities can be obtained by summing over quantum mechanical and thermal fluctuations with the help of path integrals [7,8]. In order to evaluate the path integral for the free energy approximately, Feynman and Kleinert developed a variational method in 1986 [9]. It replaces the relevant system by the exactly solvable harmonic oscillator whose frequency becomes a variational parameter that has to be optimized. Starting with Ref. [10], this method has been systematically extended by Kleinert to higher orders [5,11]. It is now known as the variational perturbation theory and yields results for all temperatures and all coupling strengths.

In Sec. X we extend this procedure to higher orders of the free energy and cross check the results in Sec. XI.

II. PATH INTEGRAL REPRESENTATION

The path integral representation for the imaginary-time evolution amplitude of a particle of mass M moving in a one-dimensional potential $V(x)$ reads [5]

$$(x_b \hbar\beta|x_a 0)=\int_{x(0)=x_a}^{x(\hbar\beta)=x_b}\mathcal{D}x\,\exp\left\{-\frac{1}{\hbar}\int_0^{\hbar\beta}d\tau\times\left[\frac{M}{2}\dot{x}^2(\tau)+V(x(\tau))\right]\right\}. \quad (1)$$

For the anharmonic oscillator potential

*Electronic address: florian.weissbach@physik.fu-berlin.de
†Electronic address: pelster@physik.fu-berlin.de
‡Electronic address: bodo.hamprecht@physik.fu-berlin.de

$$V(x)=\frac{M}{2}\omega^2x^2+gx^4, \tag{2}$$

the imaginary-time evolution amplitude (1) can be expanded in powers of the coupling constant g. Thus we obtain the perturbation series

$$(x_b\hbar\beta|x_a0)=(x_b\hbar\beta|x_a0)_\omega\left[1-\frac{g}{\hbar}\int_0^{\hbar\beta}d\tau_1\langle x^4(\tau_1)\rangle_\omega+\cdots\right], \tag{3}$$

where we have introduced the harmonic imaginary-time evolution amplitude

$$(x_b\hbar\beta|x_a0)_\omega\equiv\int_{x(0)=x_a}^{x(\hbar\beta)=x_b}\mathcal{D}x\exp\left\{-\frac{1}{\hbar}\int_0^{\hbar\beta}d\tau\times\left[\frac{M}{2}\dot{x}^2(\tau)+\frac{M}{2}\omega^2x^2(\tau)\right]\right\}, \tag{4}$$

and the harmonic path expectation value for an arbitrary functional $F[x]$,

$$\langle F[x]\rangle_\omega\equiv\frac{1}{(x_b\hbar\beta|x_a0)_\omega}\int_{x(0)=x_a}^{x(\hbar\beta)=x_b}\mathcal{D}xF[x]\times\exp\left\{-\frac{1}{\hbar}\int_0^{\hbar\beta}d\tau\left[\frac{M}{2}\dot{x}^2(\tau)+\frac{M}{2}\omega^2x^2(\tau)\right]\right\}. \tag{5}$$

The latter is evaluated with the help of the generating functional for the harmonic oscillator, whose path integral representation reads

$$(x_b\hbar\beta|x_a0)_\omega[j]=\int_{x(0)=x_a}^{x(\hbar\beta)=x_b}\mathcal{D}x\exp\left\{-\frac{1}{\hbar}\int_0^{\hbar\beta}d\tau\left[\frac{M}{2}\dot{x}^2(\tau)+\frac{M}{2}\omega^2x^2(\tau)-j(\tau)x(\tau)\right]\right\}, \tag{6}$$

leading to [5]

$$(x_b\hbar\beta|x_a0)_\omega[j]=(x_b\hbar\beta|x_a0)_\omega\times\exp\left[\frac{1}{\hbar}\int_0^{\hbar\beta}d\tau_1x_{\rm cl}(\tau_1)j(\tau_1)+\frac{1}{2\hbar^2}\int_0^{\hbar\beta}d\tau_1\int_0^{\hbar\beta}d\tau_2\times G^{(D)}(\tau_1,\tau_2)j(\tau_1)j(\tau_2)\right], \tag{7}$$

with the harmonic imaginary-time evolution amplitude

$$(x_b\hbar\beta|x_a0)_\omega=\left(\frac{M\omega}{2\pi\hbar\sinh\hbar\beta\omega}\right)^{1/2}\exp\left\{-\frac{M\omega}{2\hbar\sinh\hbar\beta\omega}\times[(x_a^2+x_b^2)\cosh\hbar\beta\omega-2x_ax_b]\right\}. \tag{8}$$

In Eq. (7) we have introduced the classical path

$$x_{\rm cl}(\tau)\equiv\frac{x_a\sinh(\hbar\beta-\tau)\omega+x_b\sinh\omega\tau}{\sinh\hbar\beta\omega} \tag{9}$$

and the Dirichlet Green's function

$$G^{(D)}(\tau_1,\tau_2)\equiv\frac{\hbar}{M\omega}\frac{1}{\sinh\hbar\beta\omega}\times[\theta(\tau_1-\tau_2)\sinh(\hbar\beta-\tau_1)\omega\sinh\omega\tau_2+\theta(\tau_2-\tau_1)\sinh(\hbar\beta-\tau_2)\omega\sinh\omega\tau_1]. \tag{10}$$

We follow Refs. [3,4] and evaluate harmonic path expectation values of polynomials in x arising from the generating functional (7) according to Wick's theorem. Let us illustrate the procedure to reduce the power of polynomials by the example of the harmonic path expectation value $\langle x^n(\tau_1)x^m(\tau_2)\rangle_\omega$.

(i) Contracting $x(\tau_1)$ with $x^{n-1}(\tau_1)$ and $x^m(\tau_2)$ leads to Green's functions $G^{(D)}(\tau_1,\tau_1)$ and $G^{(D)}(\tau_1,\tau_2)$ with multiplicity $n-1$ and m, respectively. The rest of the polynomial remains within the harmonic path expectation value, leading to $\langle x^{n-2}(\tau_1)x^m(\tau_2)\rangle_\omega$ and $\langle x^{n-1}(\tau_1)x^{m-1}(\tau_2)\rangle_\omega$.

(ii) If $n>1$, extract one $x(\tau_1)$ from the path expectation value giving $x_{\rm cl}(\tau_1)$ multiplied by $\langle x^{n-1}(\tau_1)x^m(\tau_2)\rangle_\omega$.

(iii) Add the terms from (i) and (ii).

(iv) Repeat the previous steps until only products of path expectation values $\langle x(\tau_1)\rangle_\omega=x_{\rm cl}(\tau_1)$ remain.

With the help of this procedure, we obtain to first order

$$\langle x^4(\tau_1)\rangle_\omega=x_{\rm cl}^4(\tau_1)+6x_{\rm cl}^2(\tau_1)G^{(D)}(\tau_1,\tau_1)+3G^{(D)^2}(\tau_1,\tau_1). \tag{11}$$

III. FEYNMAN DIAGRAMS

These contractions can be illustrated by Feynman diagrams with the following rules: A vertex represents the integration over τ,

$$\times=\int_0^{\hbar\beta}d\tau, \tag{12}$$

a line denotes the Dirichlet Green's function

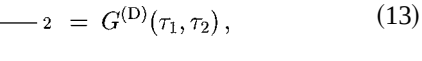

$$1\text{——}2\;=\;G^{(D)}(\tau_1,\tau_2), \tag{13}$$

and a cross or a ''current'' pictures a classical path

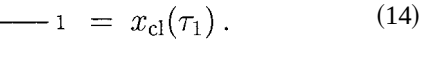

$$\times\text{——}1\;=\;x_{\rm cl}(\tau_1). \tag{14}$$

Inserting the harmonic path expectation value (11) into the perturbation expansion (3) leads in first order to the diagrams

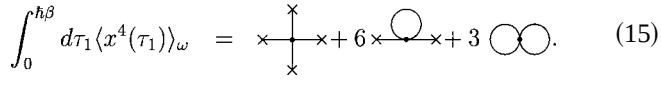

$$\int_0^{\hbar\beta}d\tau_1\langle x^4(\tau_1)\rangle_\omega\;=\;\times+6\times\bigcirc\times+3\;\bigcirc\bigcirc. \tag{15}$$

We now evaluate the first-order Feynman diagrams in Eq. (15) for finite temperatures and arbitrary x_a, x_b. Thus we will get a first-order result for the imaginary-time evolution amplitude in Eq. (3). The first diagram leads to

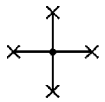

$$= \frac{1}{32\omega \sinh^4 \hbar\beta\omega} [(x_a^4 + x_b^4)(\sinh 4\hbar\beta\omega - 8 \sinh 2\hbar\beta\omega + 12\hbar\beta\omega) + (x_a^3 x_b + x_a x_b^3)(4 \sinh 3\hbar\beta\omega + 36 \sinh \hbar\beta\omega - 48\hbar\beta\omega \cosh \hbar\beta\omega) + x_a^2 x_b^2(-36 \sinh 2\hbar\beta\omega + 48\hbar\beta\omega + 24\hbar\beta\omega \cosh 2\hbar\beta\omega)], \tag{16}$$

and the second diagram reduces to

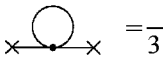

$$= \frac{\hbar}{32M\omega^2 \sinh^3 \hbar\beta\omega} [(x_a^2 + x_b^2)(\sinh 3\hbar\beta\omega + 9 \sinh \hbar\beta\omega - 12\hbar\beta\omega \cosh \hbar\beta\omega) + x_a x_b(-12 \sinh 2\hbar\beta\omega + 16\hbar\beta\omega + 8\hbar\beta\omega \cosh 2\hbar\beta\omega)], \tag{17}$$

whereas the last diagram turns out to be

$$= \frac{\hbar^2}{16M^2\omega^3 \sinh^2 \hbar\beta\omega} (-3 \sinh 2\hbar\beta\omega + 4\hbar\beta\omega + 2\hbar\beta\omega \cosh 2\hbar\beta\omega). \tag{18}$$

So, all in all, we get the following first-order result for the imaginary-time evolution amplitude:

$$(x_b \hbar\beta | x_a 0) = (x_b \hbar\beta | x_a 0)_\omega \Bigg(1 - \frac{g}{\hbar} \Bigg\{ \frac{\hbar^2}{M^2\omega^3 \sinh^2 \hbar\beta\omega} [-\tfrac{9}{16} \sinh 2\hbar\beta\omega + \tfrac{3}{4}\hbar\beta\omega + \tfrac{3}{8}\hbar\beta\omega \cosh 2\hbar\beta\omega] + \frac{\hbar}{M\omega^2 \sinh^3 \hbar\beta\omega} [(x_a^2 + x_b^2)(\tfrac{3}{16} \sinh 3\hbar\beta\omega + \tfrac{27}{16} \sinh \hbar\beta\omega - \tfrac{9}{4}\hbar\beta\omega \cosh \hbar\beta\omega) + x_a x_b(-\tfrac{9}{4} \sinh 2\hbar\beta\omega + 3\hbar\beta\omega + \tfrac{3}{2}\hbar\beta\omega \cosh 2\hbar\beta\omega)] + \frac{1}{\omega \sinh^4 \hbar\beta\omega} [(x_a^4 + x_b^4)(\tfrac{1}{32} \sinh 4\hbar\beta\omega - \tfrac{1}{4} \sinh 2\hbar\beta\omega + \tfrac{3}{8}\hbar\beta\omega) + (x_a^3 x_b + x_a x_b^3)(\tfrac{1}{8} \sinh 3\hbar\beta\omega + \tfrac{9}{8} \sinh \hbar\beta\omega - \tfrac{3}{2}\hbar\beta\omega \cosh \hbar\beta\omega) + x_a^2 x_b^2(-\tfrac{9}{8} \sinh 2\hbar\beta\omega + \tfrac{3}{2}\hbar\beta\omega + \tfrac{3}{4}\hbar\beta\omega \cosh 2\hbar\beta\omega)] \Bigg\} + \cdots \Bigg). \tag{19}$$

The imaginary-time evolution amplitude thus has the time reversal behavior

$$(x_b \hbar\beta | x_a 0) = (x_a \hbar\beta | x_b 0)^*, \tag{20}$$

while it is known that the imaginary-time evolution amplitude is real for one-dimensional problems.

IV. PARTIAL DIFFERENTIAL EQUATION

Consider the Schrödinger equation for the real-time evolution amplitude

$$i\hbar \frac{\partial}{\partial t}(x_b t | x_a 0) = -\frac{\hbar^2}{2M} \frac{\partial^2}{\partial x_b^2}(x_b t | x_a 0) + V(x_b)(x_b t | x_a 0). \tag{21}$$

In order to get a corresponding quantum statistical Schrödinger equation, we now have to change from real time to imaginary time, i.e., we have to perform the Wick rotation $t \to -i\tau$. Thus the Schrödinger equation (21) becomes

$$-\hbar \frac{\partial}{\partial \tau}(x_b \tau | x_a 0) = -\frac{\hbar^2}{2M} \frac{\partial^2}{\partial x_b^2}(x_b \tau | x_a 0) + V(x_b)(x_b \tau | x_a 0). \tag{22}$$

For both the real and the imaginary-time evolution amplitude, the initial condition reads

$$(x_b 0 | x_a 0) = \delta(x_b - x_a). \tag{23}$$

Substituting the anharmonic oscillator potential (2) into the Schrödinger equation (22), we finally get

$$\left\{-\hbar\frac{\partial}{\partial\tau}+\frac{\hbar^2}{2M}\frac{\partial^2}{\partial x_b^2}-\frac{M}{2}\omega^2x_b^2-gx_b^4\right\}(x_b\tau|x_a0)=0. \tag{24}$$

Making the ansatz

$$(x_b\tau|x_a0)=(x_b\tau|x_a0)_\omega\,A(x_b,x_a,\tau), \tag{25}$$

where $(x_b\tau|x_a0)_\omega$ is the harmonic imaginary-time evolution amplitude (8), we conclude from Eq. (24) a partial differential equation for $A(x_b,x_a,\tau)$,

$$\left\{\frac{\partial}{\partial\tau}-\frac{\hbar}{2M}\frac{\partial^2}{\partial x_b^2}+\omega\frac{x_b\cosh\omega\tau-x_a}{\sinh\omega\tau}\frac{\partial}{\partial x_b}+\frac{g}{\hbar}x_b^4\right\}\times A(x_b,x_a,\tau)=0. \tag{26}$$

We now choose our ansatz for $A(x_b,x_a,\tau)$ by introducing three expansions in g, x_a, and x_b, respectively. Also we take out the factor $\sinh^{-l}\omega\tau$, such that the ordinary differential equations for the expansion coefficients become as simple as possible,

$$A(x_b,x_a,\tau)=\sum_{n=0}^{\infty}\sum_{k=0}^{2n}\sum_{l=0}^{2k}g^n\frac{c^{(n)}_{2k|l}(\tau)}{\sinh^l\omega\tau}x_a^{2k-l}x_b^l. \tag{27}$$

In order to obtain the unperturbed result $A(x_b,x_a,\tau)=1$ for $g=0$ we need $c^{(0)}_{0|0}(\tau)=1$. The superscript n in Eq. (27) denotes the perturbative order, whereas $2k$ counts the (even) powers of the various products $x_a^ix_b^j$. The summations over the coordinates x_a, x_b can be truncated at $k=2n$, because we learn from Feynman diagrammatic considerations that the diagram with the most currents x in the nth order looks like

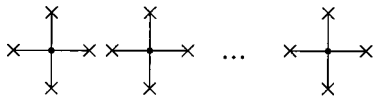

(28)

Inserting the ansatz (27) into the Schrödinger equation (26) and arranging the indices in such a way that each term is proportional to $x_a^{2k-l}x_b^l$, we get for the different powers of g and for $n>0$,

$$\begin{aligned}&\sum_{k=0}^{2n}\sum_{l=0}^{2k}\frac{x_a^{2k-l}x_b^l}{\sinh^l\omega\tau}\frac{\partial c^{(n)}_{2k|l}(\tau)}{\partial\tau}\\&-\frac{\hbar}{2M}\sum_{k=-1}^{2n-1}\sum_{l=-2}^{2k-2}(l+2)(l+1)\frac{c^{(n)}_{2k+2|l+2}(\tau)}{\sinh^{l+2}\omega\tau}x_a^{2k-l}x_b^l\\&-\omega\sum_{k=0}^{2n}\sum_{l=-1}^{2k-1}(l+1)\frac{c^{(n)}_{2k|l+1}(\tau)}{\sinh^{l+2}\omega\tau}x_a^{2k-l}x_b^l\\&+\frac{1}{\hbar}\sum_{k=2}^{2n}\sum_{l=4}^{2k+4}\frac{c^{(n-1)}_{2k-4|l-4}(\tau)}{\sinh^{l-4}\omega\tau}x_a^{2k-l}x_b^l=0.\end{aligned} \tag{29}$$

Thus the sums over k and over l collapse and we determine the master equation for our coefficients $c^{(n)}_{2k|l}(\tau)$,

$$\begin{aligned}\frac{\partial c^{(n)}_{2k|l}(\tau)}{\partial\tau}&=(l+2)(l+1)\frac{\hbar}{2M}\frac{c^{(n)}_{2k+2|l+2}(\tau)}{\sinh^2\omega\tau}\\&+(l+1)\omega\frac{c^{(n)}_{2k|l+1}(\tau)}{\sinh^2\omega\tau}\\&-\frac{1}{\hbar}c^{(n-1)}_{2k-4|l-4}(\tau)\sinh^4\omega\tau,\end{aligned} \tag{30}$$

which is solved by

$$\begin{aligned}c^{(n)}_{2k|l}(\tau)&=(l+2)(l+1)\frac{\hbar}{2M}\int d\tau\frac{c^{(n)}_{2k+2|l+2}(\tau)}{\sinh^2\omega\tau}\\&+(l+1)\omega\int d\tau\frac{c^{(n)}_{2k|l+1}(\tau)}{\sinh^2\omega\tau}\\&-\frac{1}{\hbar}\int d\tau c^{(n-1)}_{2k-4|l-4}(\tau)\sinh^4\omega\tau+d^{(n)}_{2k|l}.\end{aligned} \tag{31}$$

Here the $d^{(n)}_{2k|l}$ denote the integration constants that are fixed by applying the initial condition

$$\lim_{\tau\to0}\left|\frac{c^{(n)}_{2k|l}(\tau)}{\sinh^l\omega\tau}\right|<\infty. \tag{32}$$

However, the above master equation (30) is not valid for all k and l. Therefore, we now introduce a set of empirical rules telling us which of the coefficients $c^{(n)}_{2k|l}(\tau)$ have to be dropped once we write down (31) for any order n: (i) drop all terms containing a $c^{(n)}_{2k|l}(\tau)$ where $2k>4n$; (ii) drop all terms containing a $c^{(n)}_{2k|l}(\tau)$ with $l>2k$; and (iii) neglect all terms containing a $c^{(n)}_{2k|l}(\tau)$ with any negative indices k and l.

To convince the reader that Eq. (31) together with this procedure leads to the correct results we now reobtain our first-order result from Eq. (19). To that end we set $n=1$, such that k runs from 0 to 2 and l from 0 to 4. Fixing $k=2$ and counting down from $l=4$ to $l=0$,
we get

$$\begin{aligned}c^{(1)}_{4|4}(\tau)&=-\frac{1}{\hbar}\int d\tau c^{(0)}_{0|0}(\tau)\sinh^4\omega\tau+d^{(1)}_{4|4}\\&=\frac{1}{\hbar\omega}\left(\tfrac{1}{32}\sinh4\omega\tau-\tfrac{1}{4}\sinh2\omega\tau+\tfrac{3}{8}\sinh\omega\tau\right),\end{aligned} \tag{33}$$

$$\begin{aligned}c^{(1)}_{4|3}(\tau)&=4\omega\int d\tau\frac{c^{(1)}_{4|4}(\tau)}{\sinh^2\omega\tau}+d^{(1)}_{4|3}\\&=\frac{1}{\hbar\omega\sinh\omega\tau}\left(\tfrac{1}{8}\sinh3\omega\tau+\tfrac{9}{8}\sinh\omega\tau-\tfrac{3}{2}\cosh\omega\tau\right),\end{aligned} \tag{34}$$

$$c^{(1)}_{4|2}(\tau)=3\omega\int d\tau\frac{c^{(1)}_{4|3}(\tau)}{\sinh^2\omega\tau}+d^{(1)}_{4|2}$$
$$=\frac{1}{\hbar\omega\sinh^2\omega\tau}\left(-\tfrac{9}{8}\sinh 2\omega\tau+\tfrac{3}{2}\omega\tau+\tfrac{3}{4}\omega\tau\cosh 2\omega\tau\right), \quad (35)$$

$$c^{(1)}_{4|1}(\tau)=2\omega\int d\tau\frac{c^{(1)}_{4|2}(\tau)}{\sinh^2\omega\tau}+d^{(1)}_{4|1}$$
$$=\frac{1}{\hbar\omega\sinh^3\omega\tau}\left(\tfrac{1}{8}\sinh 3\omega\tau+\tfrac{9}{8}\sinh\omega\tau-\tfrac{3}{2}\omega\tau\cosh\omega\tau\right), \quad (36)$$

$$c^{(1)}_{4|0}(\tau)=\omega\int d\tau\frac{c^{(1)}_{4|1}(\tau)}{\sinh^2\omega\tau}+d^{(1)}_{4|0}$$
$$=\frac{1}{\hbar\omega\sinh^4\omega\tau}\left(\tfrac{1}{32}\sinh 4\omega\tau-\tfrac{1}{4}\sinh 2\omega\tau+\tfrac{3}{8}\sinh\omega\tau\right). \quad (37)$$

Correspondingly, for $k=1$, we obtain

$$c^{(1)}_{2|2}(\tau)=\frac{6\hbar}{M}\int d\tau\frac{c^{(1)}_{4|4}(\tau)}{\sinh^2\omega\tau}+d^{(1)}_{2|2}$$
$$=\frac{1}{M\omega^2\sinh\omega\tau}\left(\tfrac{3}{16}\sinh 3\omega\tau+\tfrac{27}{16}\sinh\omega\tau-\tfrac{9}{4}\omega\tau\cosh\omega\tau\right), \quad (38)$$

$$c^{(1)}_{2|1}(\tau)=\frac{3\hbar}{M}\int d\tau\frac{c^{(1)}_{4|3}(\tau)}{\sinh^2\omega\tau}+2\omega\int d\tau\frac{c^{(1)}_{2|2}(\tau)}{\sinh^2(\tau)}+d^{(1)}_{2|1}$$
$$=\frac{1}{M\omega^2\sinh^2\omega\tau}\left(-\tfrac{9}{4}\sinh 2\omega\tau+3\omega\tau+\tfrac{3}{2}\omega\tau\cosh 2\omega\tau\right), \quad (39)$$

$$c^{(1)}_{2|0}(\tau)=\frac{\hbar}{M}\int d\tau\frac{c^{(1)}_{4|2}(\tau)}{\sinh^2\omega\tau}+\omega\int d\tau\frac{c^{(1)}_{2|1}(\tau)}{\sinh^2(\tau)}+d^{(1)}_{2|0}$$
$$=\frac{1}{\hbar\omega^2\sinh^3\omega\tau}\left(\tfrac{3}{16}\sinh 3\omega\tau+\tfrac{27}{16}\sinh\omega\tau-\tfrac{9}{4}\omega\tau\cosh\omega\tau\right). \quad (40)$$

Finally for $k=0$ we get the equation

$$c^{(1)}_{0|0}(\tau)=\frac{\hbar}{M}\int d\tau\frac{c^{(1)}_{2|2}(\tau)}{\sinh^2\omega\tau}+d^{(1)}_{0|0}$$
$$=\frac{\hbar}{M^2\omega^3\sinh^2\omega\tau}\left(-\tfrac{9}{16}\sinh 2\omega\tau+\tfrac{3}{4}\omega\tau+\tfrac{3}{8}\omega\tau\cosh 2\omega\tau\right). \quad (41)$$

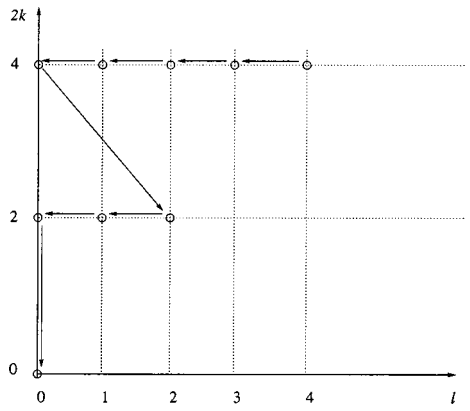

FIG. 1. This diagram depicts the path of recursion for $n=1$. We start in the top right hand corner, which is to be identified with the coefficient $c^{(1)}_{4|4}$ and follow the arrows until reaching the bottom left hand corner with the coefficient $c^{(1)}_{0|0}$.

The path of recursion, which follows from this procedure, is shown in Fig. 1.

V. EXPLOITING THE SYMMETRIES

As seen above, we already have to solve nine ordinary differential equations for the first-order imaginary-time evolution amplitude. For any order n, the number p of integrals to solve is

$$p=\sum_{j=1}^{2n+1}(2j-1)=4n^2+4n+1. \quad (42)$$

Due to the time reversal behavior (20), the coefficients $c^{(n)}_{2k|l}(\tau)$ show a symmetry, namely,

$$\frac{c^{(n)}_{2k|l}(\tau)}{\sinh\omega\tau}=\frac{c^{(n)}_{2k|2k-l}(\tau)}{\sinh^{2k-l}\omega\tau}. \quad (43)$$

Exploiting the symmetry (43), we can cut down the number (42) considerably. At first sight, it is reduced to

$$p'=\sum_{j=1}^{2n+1}j=2n^2+3n+1, \quad (44)$$

so there are only six integrals left for the first order. But we can go even further. Employing these symmetries we can eventually change almost all recursive *differential* equations into purely *algebraic* ones leaving only $p''=(2n+1)$ integrations. So, for the first order, we are left with three integrations only, namely, Eqs. (33), (38), and (41). The coefficients $c^{(1)}_{4|4}(\tau)$, $c^{(1)}_{2|2}(\tau)$, and $c^{(1)}_{0|0}(\tau)$ are integrated recursively. The other coefficients can then be obtained algebraically: Once we have $c^{(1)}_{4|4}(\tau)$, we also know $c^{(1)}_{4|0}(\tau)$ because of the symmetry (43). Comparing Eq. (31) for $k=2$, $l=4$ and $k=2$, $l=0$ we then obtain an algebraic equation for $c^{(1)}_{4|1}(\tau)$. The knowledge of $c^{(1)}_{4|1}(\tau)$ gives us $c^{(1)}_{4|3}(\tau)$ because of the symmetry (43) and by comparing Eq. (31) this time for $k=2$, $l=3$ on the one hand and $k=2$, $l=1$ on the other hand we are left with an algebraic equation for $c^{(1)}_{4|2}(\tau)$. Thus

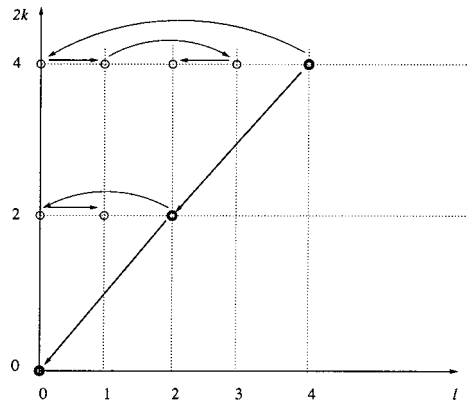

FIG. 2. This diagram shows which of the first-order coefficients $c^{(1)}_{2k|l}(\tau)$ have to be integrated (bold) and which ones can be obtained by employing symmetry and algebraic recursions (light).

we get all the coefficients for $k=2$ only by solving one differential equation, namely, the one for $c^{(1)}_{4|4}(\tau)$. For $k=1$ the procedure is similar, $k=0$ only generates one coefficient anyway, namely, $c^{(1)}_{0|0}(\tau)$, which still has to be solved by evaluating one integral. The new path of recursion is shown in Fig. 2. So finally three out of the nine first-order coefficients are obtained by integration, three more are clear for symmetry reasons, and three come from an algebraic recursion.

We now generalize the algebraic part of our recursion. Consider again the symmetry property (43). Differentiation on both sides yields

$$\frac{\partial c^{(n)}_{2k|l}(\tau)}{\partial\tau}=\frac{1}{\sinh^{2k-2l}\omega\tau}\frac{\partial c^{(n)}_{2k|2k-l}(\tau)}{\partial\tau}-2(k-l)\omega\cosh\omega\tau\frac{c^{(n)}_{2k|2k-l}(\tau)}{\sinh^{2k-2l+1}\omega\tau}. \quad (45)$$

Now we substitute for the two partial derivatives according to Eq. (30). Solving for the $(l+1)$st coefficient and shifting the index l down by 1, we obtain

$$\begin{aligned}c^{(n)}_{2k|l}(\tau)=&-\frac{(l+1)\hbar}{2M\omega}c^{(n)}_{2k+2|l+1}(\tau)+\frac{c^{(n-1)}_{2k-4|l-5}(\tau)}{\hbar\omega l}\sinh^6\omega\tau\\&+\frac{(2k-l+3)(2k-l+2)\hbar}{2M\omega l}\frac{c^{(n)}_{2k+2|2k-l+3}(\tau)}{\sinh^{2k-2l+2}\omega\tau}\\&+\frac{2k-l+2}{l}\frac{c^{(n)}_{2k|2k-l+2}(\tau)}{\sinh^{2k-2l+2}\omega\tau}\\&-\frac{1}{\hbar\omega l}\frac{c^{(n-1)}_{2k-4|2k-l-3}(\tau)}{\sinh^{2k-2l-4}\omega\tau}\\&-\frac{(2k-2l+2)\cosh\omega\tau}{l}\frac{c^{(n)}_{2k|2k-l+1}(\tau)}{\sinh^{2k-2l+1}\omega\tau}, \quad (46)\end{aligned}$$

which is the algebraic recursion relation for any nondiagonal coefficient $c^{(n)}_{2k|l}(\tau)$ with $0<l\leqslant k$. (The coefficients with $k<l<2k$ are then clear for symmetry reasons.) The diagonal coefficients $c^{(n)}_{2k|2k}(\tau)$ are yet to be integrated.

VI. COMBINED DIFFERENTIAL AND ALGEBRAIC EQUATION

We now combine the differential recursion with the algebraic one. As only the diagonal coefficients have to be evaluated by integrating the differential recursive equation, we can even further simplify the solution (31) to our master equation (30). We only need it for the diagonal coefficients, for which $l+1=2k+1$ is always greater than $2k$. And according to our index rule (ii), coefficients of the shape $c^{(n)}_{2k|2k+1}$ have to be neglected. We get

$$c^{(n)}_{2k|2k}(\tau)=(2k+2)(2k+1)\frac{\hbar}{2M}\int d\tau\frac{c^{(n)}_{2k+2|2k+2}(\tau)}{\sinh^2\omega\tau}-\frac{1}{\hbar}\int d\tau c^{(n-1)}_{2k-4|2k-4}(\tau)\sinh^4\omega\tau+d^{(n)}_{2k|2k}. \quad (47)$$

Index rules (i) and (iii) still have to be applied, k runs from 0 to $2n$.

Let us quickly summarize the combined differential and algebraic recursion relation considering the first order as an example. Figure 2 shows all first-order coefficients for the imaginary-time evolution amplitude. Each coefficient is represented by a little circle. Now the coefficients on the diagonal line $2k=l$ have to be obtained by referring to Eq. (47) together with rules (i) and (iii). These two rules tell us which of the coefficients either from the same order n or from the previous order $n-1$ have to be integrated and which ones can be put to zero.

Once we have the diagonal coefficients $c^{(n)}_{2k|2k}(\tau)$, we can calculate the off-diagonal ones with $l\leqslant k$ with the help of Eq. (46). The coefficients with $k<l<2k$ are then clear for symmetry reasons.

Using the computer algebra program MAPLE7 we managed to calculate seven perturbative orders of the imaginary-time evolution amplitude, which can be found in Ref. [12].

VII. FREE ENERGY

In this section we obtain perturbative results for the partition function by integrating the diagonal elements of our perturbative expression for the imaginary-time evolution amplitude from the previous sections,

$$Z=\int_{-\infty}^{+\infty}dx(x\hbar\beta|x0). \quad (48)$$

From the partition function we then compute the free energy perturbatively,

$$F=-\frac{1}{\beta}\ln Z. \tag{49}$$

We have to expand the logarithm in order to obtain a perturbation expansion for the free energy F. For the first order we insert Eq. (19) together with Eq. (8) into Eq. (48) and evaluate the integral, and, for the second order, we use, correspondingly, the data from Ref. [12]. By taking the logarithm we get with Eq. (49) and with the expansion for the logarithm for the free energy to second order

$$F^{(2)}(\beta)=\frac{1}{\beta}\ln 2\,\sinh\frac{\hbar\beta\omega}{2}+\frac{3g\hbar^2}{4M^2\omega^2}\coth^2\frac{\hbar\beta\omega}{2}-\frac{g^2\hbar^3}{64M^4\omega^5}\times\left(\frac{54\hbar\beta\omega}{\sinh\frac{\hbar\beta\omega}{2}}+\frac{36\hbar\beta\omega\cosh\hbar\beta\omega+60\sinh\hbar\beta\omega+21\sinh 2\hbar\beta\omega}{\sinh\frac{\hbar\beta\omega}{2}}\right). \tag{50}$$

The higher orders are omitted for the sake of keeping the type face clear. With MAPLE we came as high as the fifth perturbative order, which is two orders more than what has been obtained in Ref. [14] with Feynman diagrammatic techniques.

VIII. DIAGRAMMATICAL CHECK

It is possible to check the perturbative results for the free energy for all temperatures. Namely, we can expand Z in terms of harmonic expectations in a similar way as for the imaginary-time evolution amplitude in Eq. (3). To that end, we need the generating functional

$$Z[j(\tau)]=\int_{-\infty}^{+\infty}dx(x\hbar\beta|x0)_\omega[j], \tag{51}$$

which we get from Eqs. (7)–(10). It is of the form

$$Z[j(\tau)]=Z[0]\exp\left[\frac{1}{2\hbar^2}\int_0^{\hbar\beta}d\tau_1\int_0^{\hbar\beta}d\tau_2\times G^{(p)}(\tau_1,\tau_2)j(\tau_1)j(\tau_2)\right], \tag{52}$$

where the harmonic partition function reads

$$Z[0]=\frac{1}{2\sinh\frac{\hbar\beta\omega}{2}} \tag{53}$$

and

$$G^{(p)}(\tau_1,\tau_2)=\frac{\hbar}{2M\omega}\frac{\cosh\left(\frac{\hbar\beta\omega}{2}-|\tau_1-\tau_2|\omega\right)}{\sinh\frac{\hbar\beta\omega}{2}} \tag{54}$$

denotes the periodic Green's function of the harmonic oscillator. We now obtain the partition function Z of the anharmonic oscillator from the generating functional $Z[j(\tau)]$ by differentiating with respect to the current $j(\tau)$ while setting $j(\tau)=0$ afterwards,

$$Z=\exp\left\{-\frac{1}{\hbar}\int_0^{\hbar\beta}d\tau\,g\left[\frac{\hbar\delta}{\delta j(\tau)}\right]^4\right\}Z[j(\tau)]\Bigg|_{j=0}. \tag{55}$$

Thus, we get

$$Z=Z[0]\left\{1-\frac{3g}{\hbar}\int_0^{\hbar\beta}d\tau_1 G^{(p)^2}(\tau_1,\tau_1)+\frac{g^2}{2\hbar^2}\int_0^{\hbar\beta}d\tau_1\int_0^{\hbar\beta}d\tau_2[9G^{(p)^2}(\tau_1,\tau_1)G^{(p)^2}(\tau_2,\tau_2)+72G^{(p)}(\tau_1,\tau_1)G^{(p)^2}(\tau_1,\tau_2)G^{(p)}(\tau_2,\tau_2)+24G^{(p)^4}(\tau_1,\tau_2)]+\cdots\right\}. \tag{56}$$

In terms of Feynman diagrams this reads

$$Z = Z[0]\left[1-\frac{3g}{\hbar}\;\bigcirc\!\!\bigcirc+\frac{g^2}{2\hbar^2}\left(9\;\bigcirc\!\!\bigcirc\!\!\bigcirc\!\!\bigcirc+72\;\bigcirc\!\!\bigcirc\!\!\bigcirc+24\;\text{ 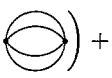 }\right)+\ldots\right] \tag{57}$$

$$=\exp\left[\frac{1}{2}\;\bigcirc-\frac{3g}{\hbar}\;\bigcirc\!\!\bigcirc+\frac{g^2}{2\hbar^2}\left(72\;\bigcirc\!\!\bigcirc\!\!\bigcirc+24\;\text{  }\right)+\ldots\right], \tag{58}$$

where we have introduced the symbol

$$\frac{1}{2}\;\bigcirc\equiv\ln\,Z[0]. \tag{59}$$

Once we rewrite the partition function Z in the form of the cumulant expansion as on the right hand side of Eq. (58), the

disconnected Feynman diagrams disappear [5]. Now we can easily take the logarithm. Following Eq. (49), we obtain for the free energy

$$F=-\frac{1}{\beta}\left[\frac{1}{2}\right.$$  $$-\frac{3g}{\hbar}$$ 
$$+\frac{g^2}{2\hbar^2}\left(72\right.$$  $$+24$$  $$\left.\left.\right)+\ldots\right]. \qquad (60)$$

The above Feynman diagrams are, of course, constructed with the help of the same rules as for the imaginary-time evolution amplitudes (12)–(14), but instead of the Dirichlet Green's function (10) we have to use the periodic Green's function (54). We now want to evaluate the four diagrams in Eq. (60) so that we get a second-order expression for the free energy for finite temperatures. According to Eqs. (53) and (59) we get for the zeroth-order contribution

$$\frac{1}{2}$$  $$=\ln\left[\frac{1}{2\sinh\frac{\hbar\beta\omega}{2}}\right], \qquad (61)$$

whereas the first-order diagram becomes

 $$=\frac{\hbar^3\beta}{4M^2\omega^2}\coth^2\frac{\hbar\beta\omega}{2}. \qquad (62)$$

The integration in Eq. (62) is trivial, because $G^{(p)}(\tau,\tau)$ does not depend on τ any more according to Eq. (54). For the second order the integrations become more sophisticated,

 $$=\frac{\hbar^5\beta\coth^2\frac{\hbar\beta\omega}{2}}{32M^4\omega^5\sinh^2\frac{\hbar\beta\omega}{2}}\times(\hbar\beta\omega+\sinh\hbar\beta\omega). \qquad (63)$$

The other contribution to the second order yields

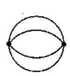 $$=\frac{\hbar^5\beta}{256M^4\omega^5\sinh^4\frac{\hbar\beta\omega}{2}}\times(\sinh 2\hbar\beta\omega+8\sinh\hbar\beta\omega+6\hbar\beta\omega). \qquad (64)$$

So all in all we get for the free energy (60) up to second order in the coupling constant g the result (50). It shows the correct low-temperature behavior

$$\lim_{\beta\to\infty}F^{(2)}(\beta)=\frac{\hbar\omega}{2}+\frac{3g\hbar^2}{4M^2\omega^2}-\frac{21g^2\hbar^3}{8M^4\omega^5}, \qquad (65)$$

which is the ground state energy and can be found, for instance, in Refs. [1,5].

IX. VARIATIONAL PERTURBATION THEORY

Variational perturbation theory is a method that enables us to resum divergent Borel-type perturbation series in such a way that they converge even for infinitely large values of the perturbative coupling [5,11]. To this end, we add and subtract a trial harmonic oscillator with trial frequency Ω to our anharmonic oscillator (2),

$$V(x)=\frac{M}{2}\Omega^2x^2+g\frac{M}{2}\frac{\omega^2-\Omega^2}{g}x^2+gx^4. \qquad (66)$$

Now we treat the second term as if it was of the order of the coupling constant g. The result is obtained most simply by substituting for the frequency ω in the original anharmonic oscillator potential (2) according to Kleinert's square-root trick [5]

$$\omega\to\Omega\sqrt{1+gr}, \qquad (67)$$

where

$$r\equiv\frac{\omega^2-\Omega^2}{g\Omega^2}. \qquad (68)$$

These substitutions are not the most general ones. The square root is just a special case for the anharmonic oscillator.

We now apply the trick (67) to our first-order series representation for the free energy F found in Eq. (50). Substituting for the frequency ω according to Eq. (67), expanding for fixed r up to the first order in g and resubstituting for r according to Eq. (68) we get

$$F^{(1)}(\beta,\Omega)=-\frac{1}{\beta}\ln\frac{1}{2\sinh\frac{\hbar\beta\Omega}{2}}+\frac{3g\hbar^2}{4M^2\Omega^2}\coth^2\frac{\hbar\beta\Omega}{2}+\frac{\hbar\Omega}{4}\left(\frac{\omega^2}{\Omega^2}-1\right)\coth\frac{\hbar\beta\Omega}{2}. \qquad (69)$$

So the free energy (69) now depends on the trial frequency Ω, which is of no physical relevance. In order to get rid of it, we have to minimize its effect by employing the principle of least sensitivity [13]. This principle suggests searching for local extrema of $F(\beta,\Omega)$ with respect to Ω,

$$\frac{\partial F^{(1)}(\beta,\Omega)}{\partial\Omega}=0. \qquad (70)$$

For the first order $F^{(1)}(\beta,\Omega)$ it turns out that there are several extrema for each β. As we seek a curve $\Omega^{(1)}(\beta)$ that is as smooth as possible, the choice is easy—we take the lowest branch for the others are not bounded (see Fig. 3). Moreover, the other branches lead to diverging results.

To second order, we proceed in a similar way and we find that there are no extrema at all for $F^{(2)}(\beta,\Omega)$. In accordance with the principle of least sensitivity we look for inflection points instead, i.e., we look for solutions to the equation

$$\frac{\partial^2F^{(2)}(\beta,\Omega)}{\partial\Omega^2}=0. \qquad (71)$$

In general, we try to solve the equation

$$\frac{\partial^nF^{(N)}(\beta,\Omega)}{\partial\Omega^n}=0 \qquad (72)$$

for the smallest possible n. Plugging $\Omega^{(N)}(\beta)$ into $F^{(N)}(\beta,\Omega)$, we finally get back a resummed expression for

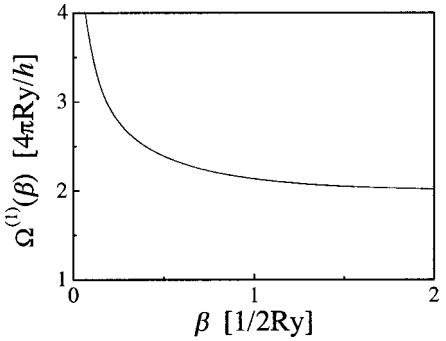

FIG. 3. Branch of the variational parameter $\Omega^{(1)}(\beta)$ chosen by us. The coupling strength is $g=1$. Other branches not shown in this figure lead to highly diverging results. Throughout this paper all results are presented in natural units $\hbar=k_B\equiv 1$ and, additionally, we have set $M=\omega\equiv 1$.

the physical quantity $F(\beta)$. The results for the first three orders are given in Fig. 4. In order to check our results, we have to compare them to the numerically evaluated free energy $F^{(N)}_{\rm num}(\beta)$ which is discussed in Sec. XI.

X. HIGHER ORDERS

We now evaluate the convergence behavior of the variational perturbative results for the free energy $F^{(N)}(\beta)$ up to the fifth order. However, in order to reduce the computational cost we restrict ourselves to a certain value of the inverse temperature β. Results are shown in Fig. 5. For odd variational perturbation orders we optimized the free energy according to Eq. (70), i.e., we determined Ω by setting the first derivative of $F^{(N)}(\beta)$ with respect to Ω to zero. For even orders we had to go for inflection points, instead, so we had to solve Eq. (71).

It turns out that odd and even orders oscillate about an exponential best fit curve. For $\beta=1$, the numerical result

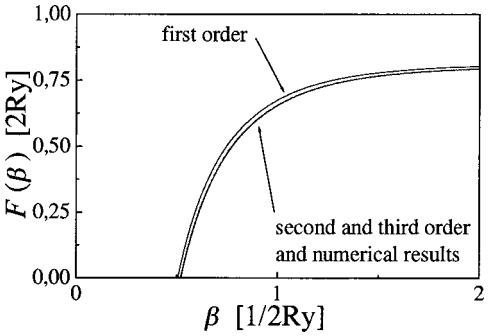

FIG. 4. Free energy of the anharmonic oscillator up to third order for intermediate coupling $g=1$. The solid line represents the numerical result $F^{(9)}_{\rm num}(\beta)$, obtained by approximating the partition function (74) with the help of the first ten energy eigenvalues. The other lines are variational perturbative results. The dashed line shows the first order, the dotted line shows the second order, and the dot-dashed line represents the third order. Note that the second and third orders are hardly distinguishable from the numerical results. Higher orders for a special value of the inverse temperature β can be found in Fig. 5.

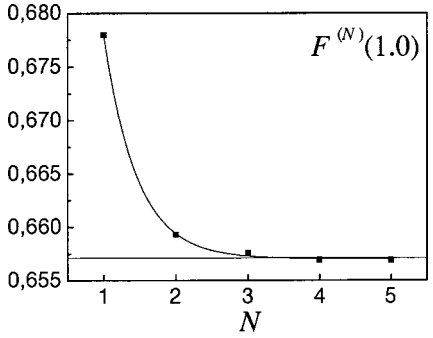

FIG. 5. The free energy of the anharmonic oscillator for intermediate coupling $g=1$ for $\beta=1$ up to the fifth variational perturbative order. The values converge exponentially towards the numerical value $F^{(9)}_{\rm num}(1)=0.6571$, which is shown as a straight line. The dimension of the free energy in natural units is 2 Ry.

$F^{(9)}_{\rm num}(1.0)=0.6571$ turns out to lie within the interval obtained by fitting the five perturbative orders of the free energy with ORIGIN, as shown in Fig. 5. This interval is [0.657, 0.659], and clearly, the variational perturbative results converge exponentially.

XI. CHECKING OUR RESULTS

The spectral representation of the partition function reads

$$Z=\sum_{n=0}^{\infty} e^{-\beta E_n}, \tag{73}$$

where the E_n are the energy eigenvalues. Let us define the numerical approximants

$$Z^{(N)}_{\rm num}=\sum_{n=0}^{N} e^{-\beta E_n} \tag{74}$$

and

$$F^{(N)}_{\rm num}=-\frac{1}{\beta}\ln Z^{(N)}_{\rm num}, \tag{75}$$

respectively. One possibility to obtain numerical results for the eigenvalues E_n is provided by the so-called "shooting method." We integrate the Schrödinger equation numerically for the potential (2) and for a particular value of the coupling strength g. If the energy E that we plug into the program does not coincide with one of the energy eigenvalues E_n, the solution to the Schrödinger equation explodes already for relatively small values of the coordinate x. If the energy eigenvalue is close to the exact answer, we have $|\Psi(x)|<\infty$ also for larger values of x. This method yields the unnormalized eigenfunctions (the wave functions which still have to be normalized) and the energy eigenvalues to very high accuracy (see Table I). Renormalization is necessary, for the computer algebra program needs an initial value $\Psi(0)$, which we set to 1. Substituting the first ten numeric energy eigenvalues into Eq. (74) and evaluating Eq. (75) up to $N=9$, we obtain a function $F^{(N)}_{\rm num}(\beta)$. It converges rapidly for low tem-

TABLE I. The first ten energy eigenvalues, E_n, of the anharmonic oscillator for intermediate coupling $g=1$. They were obtained by numerically integrating the Schrödinger equation with the initial condition that $\Psi(0)=1$, $\Psi'(0)=0$ for even n, and $\Psi(0)=0$ and $\Psi'(0)=1$ for odd n, and of course $|\Psi(x)|<\infty$ for large x. The energy eigenvalues are given in units of 2 Ry.

n	E_n	n	E_n
0	0.803 770 193 2	5	14.203 064 494
1	2.737 889 148 4	6	17.633 934 116
2	5.179 281 461 9	7	21.236 268 598
3	7.942 380 454 4	8	24.994 705 012
4	10.963 538 555	9	28.896 941 521

peratures, corresponding to high values of β. For high temperatures more terms should be taken into account.

Alternatively, one can also use classical results as a high-temperature cross check: High temperatures correspond to classical statistical distributions such that we can evaluate the classical partition function according to

$$Z_{\mathrm{cl}}=\int_{-\infty}^{+\infty}\frac{dx}{\lambda_{\mathrm{th}}}\exp[-\beta V(x)], \tag{76}$$

with the potential (2) and $\lambda_{\mathrm{th}}=\sqrt{2\pi\hbar^2/Mk_BT}$. This integral reduces to

$$Z_{\mathrm{cl}}=\frac{1}{2\lambda_{\mathrm{th}}}\sqrt{M\omega^2/2g}\,\exp\left(\frac{\beta M^2\omega^4}{32g}\right)K_{1/4}\left(\frac{\beta M^2\omega^4}{32g}\right), \tag{77}$$

where $K_{1/4}(z)$ is a modified Bessel function. The classical partition function (77) can be evaluated for high temperatures, which corresponds to small values of β. Consequently, when we test our variational perturbative results, we compare them to the classical free energy for low values of β, namely, $\beta<\frac{1}{4}$. And for high values of β we use the numerical approximation, $F^{(9)}_{\mathrm{num}}(\beta)$, for comparison (see Fig. 6).

In natural units $\hbar=k_B=1$ a value of $\beta=\frac{1}{4}$ corresponds to a physical temperature of $T=1.26\times10^6$ K.

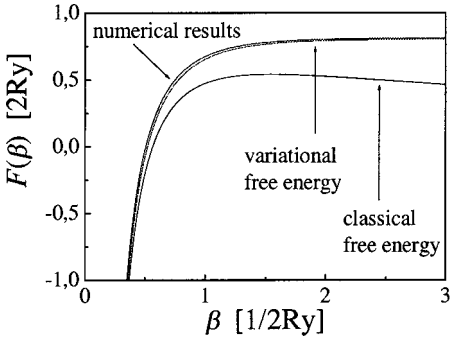

FIG. 6. The numerical free energy $F^{(9)}_{\mathrm{num}}(\beta)$, the first-order variational perturbative results for the free energy $F^{(1)}(\beta)$, and the classical free energy $F_{\mathrm{cl}}(\beta)=-(\ln Z_{\mathrm{cl}})/\beta$, from top to bottom. For small values of the inverse temperature β the classical calculations coincide with the other results. Lower temperatures, corresponding to higher values of β, reveal differences between the classical approach (77) and quantum statistics.

XII. CONCLUSION AND OUTLOOK

The recursive technique that has been developed throughout Secs. IV–VI definitely out classes all diagrammatical perturbative calculations. Using the conventional evaluation of Feynman diagrams, the partition function and the free energy have been evaluated up to third order [14]; here we obtained the fifth-order result.

For the free energy the convergence of the variational perturbation theory was found to be exponential. The fact that the principle of least sensitivity [13] produces extrema for the odd variational orders and inflection points for even orders is reflected in the respective convergence behaviors: Odd and even orders can best be fitted separately by exponentials as emphasized in Ref. [11]. Thus, we obtained intervals of convergence for certain values of the free energy, which always turned out to contain the exact numerical result when taking into account the statistical errors associated with the boundaries of the intervals. For the free energy, the numerical results were obtained using its spectral representation reverting on the first ten energy eigenvalues obtained with the shooting method, sketched in Sec. XI. Finally, we note that our high-order perturbative results for the anharmonic imaginary-time evolution amplitude are useful for calculating other thermodynamic quantities as the correlation function or the ground state wave function [3,15,16]. Furthermore, it remains to compare these perturbative results with the semiclassical approximation [17].

ACKNOWLEDGMENTS

The authors wish to thank Professor Kleinert for fruitful discussions on the variational perturbation theory.

[1] C. M. Bender and T. T. Wu, Phys. Rev. **184**, 1231 (1969); Phys. Rev. D **7**, 1620 (1973).
[2] W. Janke and H. Kleinert, Phys. Rev. Lett. **75**, 2787 (1995).
[3] A. Pelster and F. Weissbach, in *Fluctuating Paths and Fields—Festschrift Dedicated to Hagen Kleinert on the Occasion of his 60th Birthday*, edited by W. Janke, A. Pelster, H.-J. Schmidt, and M. Bachmann (World Scientific, Singapore, 2001), p. 315.
[4] H. Kleinert, A. Pelster, and M. Bachmann, Phys. Rev. E **60**, 2510 (1999).
[5] H. Kleinert, *Path Integrals in Mechanics, Statistics, Polymer Physics, and Finance*, 3rd ed. (World Scientific, Singapore, 2002).
[6] R. P. Feynman, Rev. Mod. Phys. **20**, 367 (1948).
[7] R. P. Feynman and A. R. Hibbs, *Quantum Mechanics and Path*

Integrals (McGraw-Hill, New York, 1965).
[8] R. P. Feynman, *Statistical Mechanics* (Benjamin, Reading, MA, 1972).
[9] R. P. Feynman and H. Kleinert, Phys. Rev. A **34**, 5080 (1986).
[10] H. Kleinert, Phys. Lett. A **173**, 332 (1993).
[11] H. Kleinert and V. Schulte-Frohlinde: *Critical Properties of ϕ^4-theories* (World Scientific, Singapore, 2001).
[12] The expansion coefficients $c^{(n)}_{2k|l}(\tau)$ up to the seventh order can be found at
http://www.physik.fu-berlin.de/~weissbach/coeff.html
[13] P. M. Stevenson, Phys. Rev. D **23**, 2916 (1981).
[14] H. Kleinert and H. Meyer, Phys. Lett. A **184**, 319 (1994).
[15] G. C. Rossi and M. Testa, Ann. Phys. (N.Y.) **148**, 144 (1983).
[16] T. Hatsuda, T. Kunihiro, and T. Tanaka, Phys. Rev. Lett. **78**, 3229 (1997).
[17] C. A. A. de Carvalho, R. M. Cavalcanti, E. S. Fraga, and S. E. Jorás, Phys. Rev. E **61**, 6392 (2000).